Geology and vegetation control landsliding on forest-managed slopes in scarplands

Daniel Draebing[1,2], Tobias Gebhard[1], Miriam Pheiffer[1]

[1]Chair of Geomorphology, University of Bayreuth, Bayreuth, 95447, Germany
[2]Department of Physical Geography, Utrecht University, Utrecht, 3584 CB, Netherlands

Correspondence to: Daniel Draebing (d.draebing@uni-bayreuth.de)

Abstract. Landslides are important agents of sediment transport, cause hazards and are key agents for the evolution of scarplands. Scarplands are characterized by high-strength layers overlying low-inclined landslide-susceptible layers that precondition and prepare landsliding on geological time scales. These landslides can be reactivated and their role in past hillslope evolution affected geomorphometry and material properties that set the framework for present-day shallow landslide activity. To manage present-day landslide hazards in scarplands, a combined assessment of deep-seated and shallow landsliding is required to quantify the interaction between geological conditions and vegetation that control landslide activity. For this purpose, we investigated three hillslopes affected by landsliding in the Franconian scarplands. We used geomorphic mapping to identify landforms indicating landslide activity, electrical resistivity to identify shear plane location and a mechanical stability model to assess the stability of deep-seated landslides. Furthermore, we mapped tree distribution, quantified root area ratio and root tensile strength to assess the influence of vegetation on shallow landsliding. Our results show that deep-seated landslides incorporate rotational and translational movement and suggest that sliding occurs along a geologic boundary between permeable Rhätolias sandstone and impermeable Feuerletten clays. Despite low hillslope angles, landslides could be reactivated when high pore pressures could develop along low-permeable layers. In contrast, shallow landsliding is controlled by vegetation. Our results show that rooted area is more important than species dependent root tensile strength and basal root cohesion is limited to the upper 0.5 m of the surface due to geologically controlled unfavourable soil conditions. Due to low slope inclination, root cohesion can stabilize landslide toes or slopes undercut by forest roads, independent of potential soil cohesion, when tree density is sufficient dense to provide lateral root cohesion. In summary, geology preconditions and prepares deep-seated landslides in scarplands, which set the framework of vegetation-controlled shallow landslide activity.

1 Introduction

Landslides are important agents of sediment transport, cause hazards and are key agents for the evolution of scarplands. On geological scale, sedimentary deposition in terrestrial or marine environments resulted in alternating layers of different rock strength with varying inclination (Duszyński et al., 2019), which preconditions slope stability (McColl, 2022). Horizontal

layering promotes the formation of plateaus, while tilted layers create cuestas (Young et al., 2000; Duszyński et al., 2019). Due to the differences in rock strength and resulting different efficacy of erosive processes, scarplands are characterized by high-strength layers overlying weaker sedimentary layers (Duszyński et al., 2019). Tectonic processes can increase slope height or slope steepness and erosion (e.g. by rivers) can undercut hillslopes and expose weaker sedimentary layers, which act as potential failure surfaces, and, thereby prepare landslide processes (McColl, 2022). Landslides can be caused by a wide range of triggers including e.g. rapid increase in pore water pressure by rainfall and/or snowmelt, loading of slope by precipitation or vegetation (McColl, 2022). The tilting of sedimentary layers controls the landslide type in scarplands. On frontscarps, sediment layers dip into the slope (Duszyński et al., 2019) and landslides in form of rockfall (e.g. Glade et al., 2017) or deep-seated landslides (e.g. Jäger et al., 2013) are abundant. In contrast, sedimentary layers dipping out of the slope characterize backscarps (Schmidt and Beyer, 2003; Duszyński et al., 2019), where landsliding processes comprise cambering (Hutchinson, 1991), block gliding (Young, 1983), lateral spreading (Spreafico et al., 2017) or deep-seated sliding processes (Pain, 1986; Schmidt and Beyer, 2003). Geologic conditions precondition landsliding and the formation of scarplands on geological scale. On present-day, reactivation of deep-seated landslides by geomorphic and anthropogenic processes (McColl, 2022) cause hazards to communities living in scarplands (Thiebes et al., 2014; Wilfing et al., 2018), therefore, an understanding of geologic controls on landsliding is required to analyse slope stability for hazard management.

As deep-seated landslides were important in shaping scarplands, they changed the geomorphometry of hillslopes (e.g. inclination) and sheared material and, therefore, precondition and prepare present-day shallow landslides. Shallow landslides are characterized by soil material <2 m deep moving downslope in a flowing, sliding or complex type of movement (Sidle and Bogaard, 2016; Vergani et al., 2017). Forests can affect shallow landsliding mechanically and hydrologically (Vergani et al., 2017). They can reduce soil moisture by interception and evaporation, suction and transpiration as well as infiltration and subsurface flow (Sidle and Bogaard, 2016; Vergani et al., 2017). Mechanically, forests can reinforce soil by roots (Wu, 1984; Phillips et al., 2021), roots and stems can induce buttressing (Vergani et al., 2017) and anchoring and trees can increase normal force on slopes (Ziemer, 1981; Terwilliger and Waldron, 1991; Selby, 1993; Schmidt et al., 2001; Roering et al., 2003). In forest management, the protective function of forests has been considered for a long time in high mountain regions (Dorren et al., 2005; Bischetti et al., 2009). However, forestry is not only affected by landslide activity, which causes damage to roads and loss of timber (Sidle and Ochiai, 2006), but also has a considerable impact on slope stability through changing the characteristics of forests in sliding-prone areas (Phillips et al., 2021). Root reinforcement of slope stability declines after logging operations (Ziemer, 1981; Schmidt et al., 2001; Vergani et al., 2017) and forestry roads enhance landsliding through undercutting slopes (Borga et al., 2005; van Beek et al., 2008). Changes in tree species composition and tree density have also an impact on the root reinforcement in forests (Roering et al., 2003; Genet et al., 2008). The influence of vegetation on landslides has been intensely studied on steep slopes in the European Alps (Bischetti et al., 2009; Vergani et al., 2014), the Oregon Coast Range (Schmidt et al., 2001; Roering et al., 2003), Southern California (Terwilliger and Waldron, 1991), Northern Italy (Borga et al., 2005; Schwarz et al., 2010b), New Zealand (Giadrossich et al., 2020) or China (Genet et al., 2008), however, little effort was conducted to understand the influence of vegetation on landsliding on lower-inclined hillslopes such

as scarplands in Southern Germany (e.g. Thiebes et al., 2014) or in the Flemish Ardennes (e.g. Van Den Eeckhaut et al., 2009), where geologic conditions such as clay layers enable landsliding (Skempton, 1964; Chandler, 2000; Bromhead, 2013).

As geological conditions control deep-seated landslide activity on geological scale that set the framework for shallow landslides in scarplands on present-day scale, there is a need to understand how landslide historicity affects current deep-seated and shallow landslide activity. As climate change affects forests (e.g. Seidl et al., 2017) and alters landslide activity (e.g. Crozier, 2010), combined forestry management and hazards approaches on shallow landslides (Phillips et al., 2021) should be extended by incorporating geological controls in scarplands. In this study, we aim to (1) quantify the relation between deep-seated landslides and geology in the Franconian Alb and estimate if landslides can be reactivated by hydrologic conditions. For this purpose, we extended a landslide inventory and compared landslide occurrence to geology. On three landslides, we applied electrical resistivity tomography (ERT) to identify shear plane depth and modelled hillslope stability with different water level scenarios. Furthermore, we (2) test if vegetation-induced root cohesion can stabilize shallow landslides occurring on deep-seated landslides. For this reason, we mapped tree distribution, quantified root cohesion and applied a slope stability model. Our results aim to improve forest management practices to reduce landslide occurrence in the Franconian Alb.

2 Study area

The research area is located in Northern Bavaria, Germany (Fig. 2A). Geologically, it is situated at the north-eastern margin of the Franconian Alb, which is the backscarp part of the scarplands in south Germany that consists of sand-, clay- and limestone of mostly Mesozoic age dipping gently to the East, Southeast and South (Kany and Hammer, 1985; Peterek and Schröder, 2010). Tributaries of the Red Main River eroded deep valleys into the hillslopes that consist of Middle Triassic to Lower Jurassic clay- and sandstones (Fig. 1a). The lower part of the hillslopes are formed by claystones called Feuerletten that are part of the Trossingen Formation and were deposited during prolonged flooding events in the Middle Triassic (Emmert, 1977). They are characterized by red violet, fine sandy clay- and clay-marlstones, which are weathered near surface into clay. The clay minerals consist of smectite, sudoite and illite (Emmert, 1977) with high swelling potential (Wilfing et al., 2018), impermeable and serving as an aquiclude (Boley Geotechnik, 2018). Silty and sandy lenses lead to inhomogeneities and highly varying mechanical parameters (Wilfing et al., 2018). The Feuerletten are overlain by a sequence of sand- and claystones, which are part of the Exter-Formation (Upper Triassic) and Bayreuth-Formation (Lower Jurassic). The strata are embraced as Rhätolias and the sandstones form the escarpment in the scarplands (Fig. 1a). The Exter-Formation consists of a pronounced spatial heterogeneous sequence of sandy and clayey deposits, which vary greatly in their thickness. The predominant dark-coloured clays are characterised by the occurrence of montmorillonite and kaolinite (Emmert, 1977) with high swelling capacity that can promote the formation of sliding surfaces (Wilfing et al., 2018). Intercalated quarzitic sandstone layers are predominant fine- to coarse-grained with fluviatile cross bedding (Meyer and Schmidt-Kaler, 1996). The Bayreuth-Formation is formed by a mostly massy, coarse-grained and light-coloured sequence of sandstones with a cross-bedding structure and intercalated subordinate clayey lenses (Emmert, 1977). The Rhätolias strata serves as aquifer over the Feuerletten clays that

significantly reduce the hydraulic permeability and are interpreted as sliding planes of abundant landslides (Kany and Hammer, 1985). The intense fracturing of the sandstones, due to the tectonic strain near the Franconian line, allows water to penetrate into the soil and leads to the formation of sliding surfaces along the clayey layers (Wilfing et al., 2018). The climate in the research area is warm-moderate with an annual precipitation around 719 mm and an annual temperature about 8.9 °C for the period 1991 to 2020 (DWD Climate Data Center, 2022b, a).

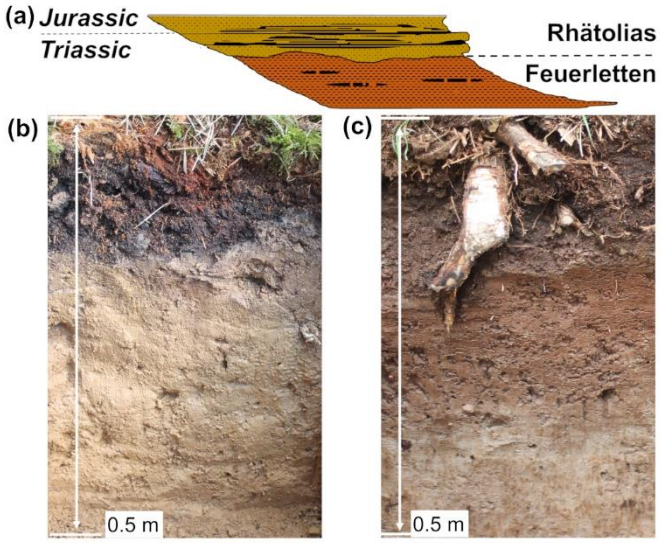

Figure 1: (a) Geological profile of investigated slopes in the Franconian Alb. Soil pits showing the upper 0.5 m of soil developed in (b) Rhätolias sandstone and (c) Feuerletten clay.

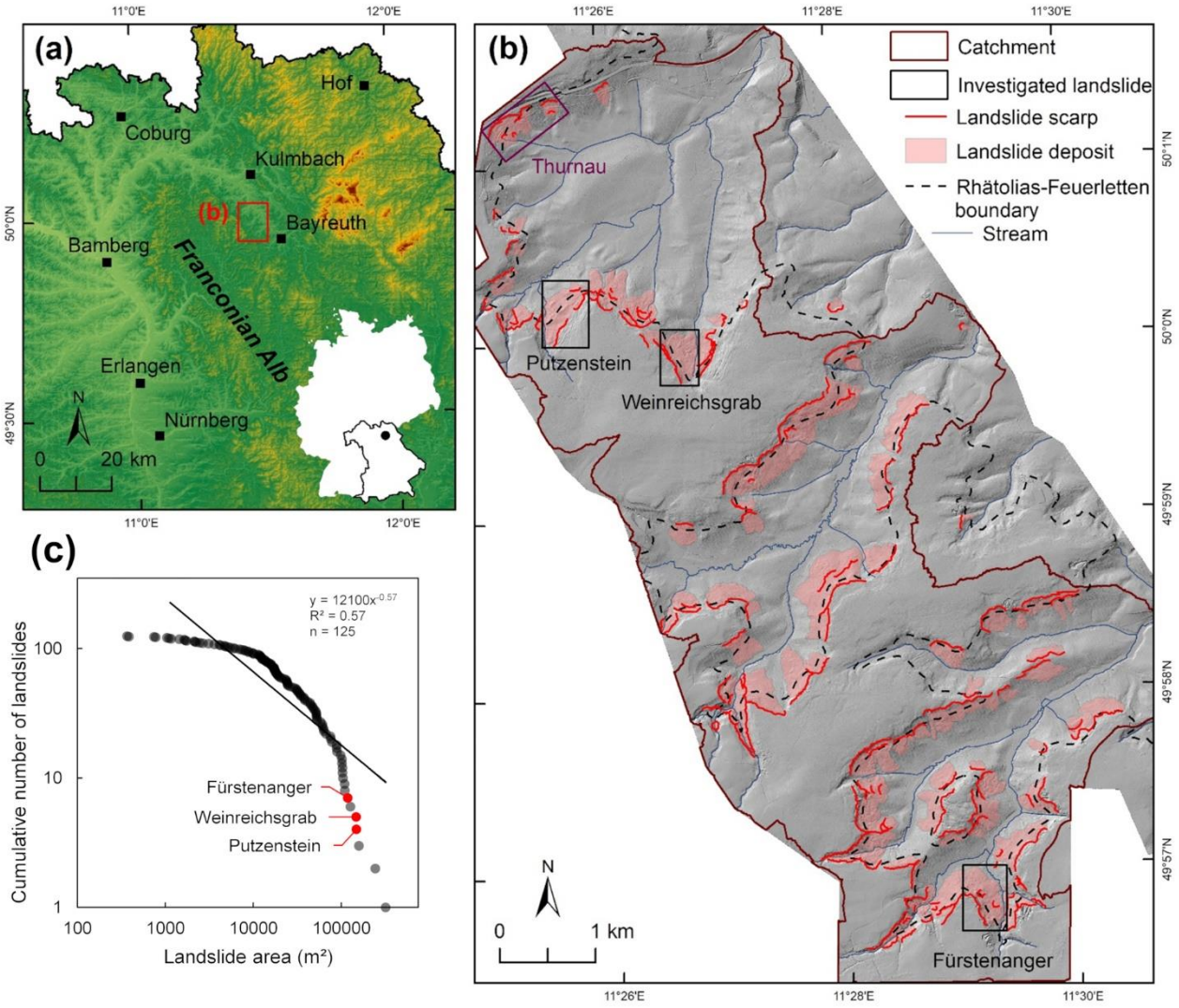

Figure 2: (a) Location of the research area at the Franconian Alb (source: Bayerisches Landesamt für Digitalisierung, Breitband und Vermessung). (b) mapped landslides based on Bayerisches Landesamt für Umwelt (2015) and own mapping including investigated landslides (source: Bayerisches Landesamt für Digitalisierung, Breitband und Vermessung). (c) Frequency-magnitude relationship of landslides.

3 Methods

3.1 Geomorphic and geologic characterisation

On regional scale (Fig. 2b), we revised the existing landslide inventory by Bayerisches Landesamt für Umwelt (2015) for our research area and mapped additional landslides based on a Digital Elevation Model (DEM) with a resolution of 1 m. To analyse

the role of geology, we derived the boundary between Rhätolias and Feuerletten from existing geological maps (Bayerisches Geologisches Landesamt, 1955, 1977, not yet published). We created a frequency-magnitude relationship based on our landslide inventory (Fig. 2c).

On local scale, geomorphic mapping was conducted in the field on three landslides with focus on landslide-induced landforms and geomorphic maps were created in ArcGIS 10.7.1 (Fig. 3). We used a longitudinal transect that started in un-affected terrain above the headscarp, went across the landslide down to or across the stream. Along this transect, we conducted 1 m long Pürckhauer soil coring with 25 to 35 m spacing to analyse the soil texture according to Ad-hoc-AG Boden (2005).

3.2 Electrical Resistivity Tomography

Electrical resistivity tomography (ERT) is a standard technique to investigate landslides (Perrone et al., 2014). The technique is well suited to differentiate landslide thickness in lithologies producing contrasting resistivities such as mudstone and sandstone (Chambers et al., 2011; Uhlemann et al., 2017) or loess and tertiary clayey sands (Van Den Eeckhaut et al., 2007). To investigate three landslides, we applied ERT along the 360 to 400 m longitudinal transects using an ABEM Terrameter LS2. We measured a Wenner array with 5 m spacing of electrodes, which enabled a penetration depth of 60 to 70 m. For data processing, we used a robust least-squared inversion in Geotomo Res2DInv (Loke and Barker, 1995). Model results showed a low root mean square (RMS) error between 5.3 and 5.4% for Putzenstein and Weinreichsgrab and an increased RMS error of 12.1% at Fürstenanger. RMS values are comparable to previous investigations identifying shear planes at clayey sand layers in the Flemish Ardennes (Van Den Eeckhaut et al., 2007; RMS 4.1 - 14.5 %) or clay layers in the Apennine (Lapenna et al., 2005; RMS 2.3 - 15.1 %). The uncertainty analysis revealed highest uncertainties near to the surface (Figure S1) and uncertainties between 1 and 5 % at our area of interest, the potential shear plane. A minimum and maximum analysis showed that ERT results are consistent (Figure S2) and data processing was not affecting the results. We used virtual 1D-ERT boreholes to identify the shear plane depth (Siewert et al., 2012) and applied a minimum, mean and maximum shear plane depth scenarios (Figure S3) for our landslide stability model.

3.3 Tree mapping and influence on stability

We mapped trees up to a lateral distance of 5 m along our approximately 400 m long ERT transects. Tree mapping included location and tree species of trees larger than 4 m. Dead and cut trees were excluded as the influence of roots on cohesion decreases with ongoing decomposition (Vergani et al., 2014; Zhu et al., 2020) until trees rot away (Ziemer, 1981; Ammann et al., 2009). At different positions along our transects, we selected individual 15 free-standing trees with a diameter at breast height (DBH) between 30 and 45 cm to minimize variations in root stability due to different growth and age (Deljouei et al., 2020). We dug 0.5 m wide and 0.5 m deep soil pits in 0.8 m distance downslope of the stem (Ji et al., 2012) of trees reflecting the three main tree species of the area: Norway spruce, Scots pine, and European beech. To determine the root area ratio

(RAR), we took photos of each soil pit, georeferenced the photos in ArcGIS 10.7.1 using tie points designated by measurement tapes in both vertical and horizontal directions, mapped every visible root and determined location and diameter (Vergani et al., 2014; Hales and Miniat, 2017). Roots with a diameter <1 mm were excluded to avoid uncertainties and roots with a diameter >10 mm were neglected as they do not contribute to the tensile strength of roots due to their stiffness (Bischetti et al., 2009; Vergani and Graf, 2016). To analyse RAR depending on depth, the profile wall was divided into 10 cm depth intervals and RAR was calculated:

$$RAR = a_r = \frac{\sum_{i=1}^{i} A_{ri}}{A} \quad (1)$$

with the root cross-sectional area A_r is

$$A_r = \frac{\pi}{4} d^2, \quad (2)$$

root diameter d and A the area of each 0.1 m segment of the soil pit. To measure root tensile strength of Scots Pine, root samples with different diameters and a minimum length of 10 cm were extracted. Sampled roots were watered for one hour to compensate for different moisture content and to ensure tensile strength measurement under wet conditions (Hales et al., 2013). Tensile strength measurements were performed applying the set-up by Hales et al. (2013) using a spring scale (G&G OCS-XY) with 0.01 kg resolution suspended with a rope on a horizontal branch. The roots were clamped using a grip tong and vertically pulled downwards until breakage using a pincer. The weight at breakage was recorded and the root diameter at breakage measured using a digital calliper (Preciva) with a resolution of 0.01 mm. Only tests with a root breakage near the middle were used for the statistical analysis (Genet et al., 2005; Bischetti et al., 2009). The force at failure FF_r was calculated from the recorded weight w:

$$FF_r = w\ g \quad (3)$$

with g is the gravitational acceleration. The root tensile strength T_r was calculated following previous studies (Schmidt et al., 2001; Genet et al., 2005):

$$T_r = \frac{FF_r}{A_r}. \quad (4)$$

A power-law between root tensile strength and root diameter d can be established for Scots pine:

$$T_r(d) = \alpha d^{-\beta} \quad (5)$$

with α and β are empirical constants depending on species. In addition, power laws for Norway spruce ($18.10\ d^{-0.72}$, $r^2 = 0.52$) and European beech ($41.57\ d^{-0.98}$, $r^2 = 0.65$) established by Bischetti et al. (2009) were used in our analysis.

The total root tensile strength t_r across the profile wall can be calculated incorporating the RAR for ith root diameters ranging from 1 to 10 mm (Bischetti et al., 2009):

$$t_r = \sum_{i=1}^{n} (T_r a_r)_i \quad (6)$$

with n is the number of roots per diameter class i. The root cohesion c_r was calculated following previous studies (Waldron, 1977; Wu, 1984; Schmidt et al., 2001):

$$c_r = (cos\alpha\ tan\emptyset + sin\alpha)\ t_r = k' t_r \quad (7)$$

with α is the angle of root deformation from the vertical angle by shearing (see Fig. 2 in Schmidt et al., 2001) and φ as the angle of internal friction of the soil. For roots with 40°< α <70° and 25°< ϕ < 40, k' is around 1.2 (Wu et al., 1979). Applying Eq. 7 with α similar to Wu et al. (1979) to the angle of internal friction for Feuerletten (Table 1) k' is around 1, which is in accordance to Bischetti et al. (2009). To consider for non-simultaneous root breakage, the correction factor k'' in the order of 0.5 was applied following Bischetti et al. (2009):

$$c_r = k'k''t_r. \quad (8)$$

Root cohesion can be differentiated into basal and lateral root cohesion (Schwarz et al., 2010a). The basal root cohesion is characterized by roots crossing the shear plane of landslide at a depth *z*. Following Bischetti et al. (2009), Eq. 6 can be adapted to

$$c_{bas}^z = (k'k'' \sum_{i=1}^{N} (T_r a_r)_i)_z \quad (9)$$

with *N* is the number of roots at a given depth.

The lateral root cohesion results from roots intersecting the vertical plane of a detachment scarp:

$$c_{lat}^z = \sum_{j=1}^{M} \left[k'k'' (\sum_{i=1}^{N} (T_r a_r)_i)_j \frac{\Delta z_j}{z} \right] \quad (10)$$

with *M* is the number of depth classes of thickness Δz_j.

The total root cohesion is the sum of basal and lateral root cohesion

$$c_r^z = c_{bas}^z + c_{lat}^z. \quad (11)$$

3.4 Landslide stability model

Mechanical strength parameters of Feuerletten and Rhätolias were quantified using approximately 90 circular, direct and triaxial tests on materials derived from 35 boreholes on the Thurnau landslide affecting the highway (Fig. 2B) and surrounding bedrock (Boley Geotechnik, 2018; Wilfing et al., 2018).

Table 1. Strength parameters according to Boley Geotechnik (2018) measured at A70 (Fig. 2b) with cohesion c'_s, angle of friction ϕ and residual angle of friction ϕ'_R.

Geology	**Soil**	c'_s **(kPa)**	Φ **(°)**	Φ'_R **(°)**
Rhätolias	Clay/silt layers	24.4 – 99.4	15.8 – 30.7	10.0 – 27.1
	Sand-gravel	0.1 – 6.6	23.1 – 38.1	
	Sand (baked)	82.9 – 102.1	24.0 – 28.6	20.5
	Median	48	23.1	13.8
	25% quantile	24.4	18.9	10.4
Upper Feuerletten	Silty clay (stiff)	49.0 – 126.0	13.4 – 24.1	
	Silty clay (soft)	11.3 – 45.9	13.4 – 26.4	8.4
	Silty clay (baked)	17.5 – 28.9	18.8 – 25.7	
	Claystone	94.9	20.1	
	Median	47.5	19.0	
	25% quantile	27.9	16.0	

To assess the reactivation of identified landslides, we used the method of slices following Fellenius (1936) and calculated the factor of safety F:

$$F = \frac{\sum_{i=1}^{n}[c'_{si}\, l_i + (W_i \cos\beta_i - \mu_i\, l_i)\tan\emptyset_i]}{\sum_{i=1}^{n}[W_i \sin\beta_i]} \quad (12)$$

with i is the number of slices, c'_s is the soil cohesion, l is the base length of each slice and β is the angle of failure plane (Selby, 1993). For each slice, W_i needs to be calculated:

$$W_i = \gamma_s z_i B_i \quad (13)$$

with γ_s is the specific weight of Feuerletten or Rhätolias in the order of 21 kN m^{-3} (Boley Geotechnik, 2018) and B_i is the width of each slice. The depth z_i and the angle of the failure plane β_i of each slice, we derived from the ERT and applied an upper, mean and lower depth to incorporate uncertainties associated with the applied geophysical technique.

The pore water pressure μ_i is calculated for each slice:

$$\mu_i = \gamma_w\, m\, z_i\, \cos^2\theta \quad (14)$$

with γ_w is the specific weight of water assuming a water density of 997 kg m^{-3} and θ is the slope angle. The slope angle θ was derived from the DEM. As the saturation is unknown, we scaled saturation using

$$m = \frac{H}{z} \quad (15)$$

with H is the height of the water table. We calculated stability scenarios from no saturation (m = 0) to full saturation (m = 1; Table 2). Where F<1, the slope is in condition of failure, while slopes with F>1 are considered as stable (Selby, 1993).

Table 2. Factor of safety scenarios for the reactivation of the entire landslide. L, m, u refer to lower, mean and upper shear plane depth scenario.

Scenario	z (m)	c'_s (kPa)	Φ (°)	m (m/m)
1 (blue)	l, m, u	28.6	8.4	0 - 1
2 (yellow)	l, m, u	8.5	8.4	0 - 1
3 (green)	l, m, u	0	8.4	0 - 1

To assess the susceptibility of shallow landsliding at undercut areas or at landslide toes, we used the infinite slope model by Skempton and De Lory (1957):

$$F = \frac{c'_s + c_r^z + (\gamma_s - m\gamma_w) z \cos^2\theta \tan\emptyset}{\gamma_s z \sin\theta \cos\theta}. \quad (16)$$

We calculated the factor of safety for cohesion scenarios ranging from no cohesion to 10 kPa assuming full saturated conditions (m=1) and a residual angle of friction of 8.4° to test if root cohesion would be sufficient to stabilize the soil.

4 Results

4.1 Geomorphology of the landslides

In our research area, 125 landslides were identified (Fig. 2b) with an area ranging from 745 m² to 320,220 m² (Fig. 2c). Around 95 % of the landslides are crossed by the Rhätolias-Feuerletten boundary (Fig. 2b). The cumulative number of landslides plotted against area showed a typical distribution with a decreasing number of landslides with increasing landslide size (Fig. 2c). We mapped three of the largest ten landslides in detail. All three landslides are characterized by the location of the headscarp within the Rhätolias formation. The Putzenstein landslide has a 710 m long headscarp and a length of up to 310 m resulting in an area of approximately 150,000 m² (Fig. 3a). Several secondary scarps and depressions are located above the headscarp without indicators of recent movement (e.g. bent trees). Within the northern most headscarp part, we observed roots that were under tension (Fig. 4a-c). The landslide area is very hummocky and the landslide front has a height between 1 and 2 m. The Weinreichsgrab landslide is characterized by a 490 m long headscarp, a length between 110 m and 330 m and an area of 120,000 m² (Fig. 3b). The headscarp exposed partially 10 - 15 m vertical sandstones (Fig. 4d) in contrast to 45° inclined slopes (Fig. 4e). The landslide area is hummocky and the front characterized by tilted and bent trees (Fig. 4f). The Fürstenanger landslide has a 490 m long headscarp (Fig. 3c) with a 10-15 m high 45° inclined slope (Fig. 4g-h). The landslide is up to 290 m long and comprises an area of 150,000 m². The upper third of the landslide area is hummocky and the landslides developed into a straight slope ending at the river (Fig. 3c). At Putzenstein landslide, fine and silty sand was abundant in the first 300 m

transect length. At 325 m transect length, reddish clays underlay a 0.2 m thick sand layer. A similar pattern was visible at Weinreichsgrab with silty and fine sand were abundant until 320 m transect length, where clays underlain a 30 to 50 cm thick sand layer. At Fürstenanger, silty and fine sand occurred until 180 m transect length. First layers of clay overlain by silty sand were observed at 24 to 40 cm depth between 181 and 206 m transect length. Clays were abundant at the surface from 236 m on but usually overlain by a 20-40 cm thick organic and silt layer.

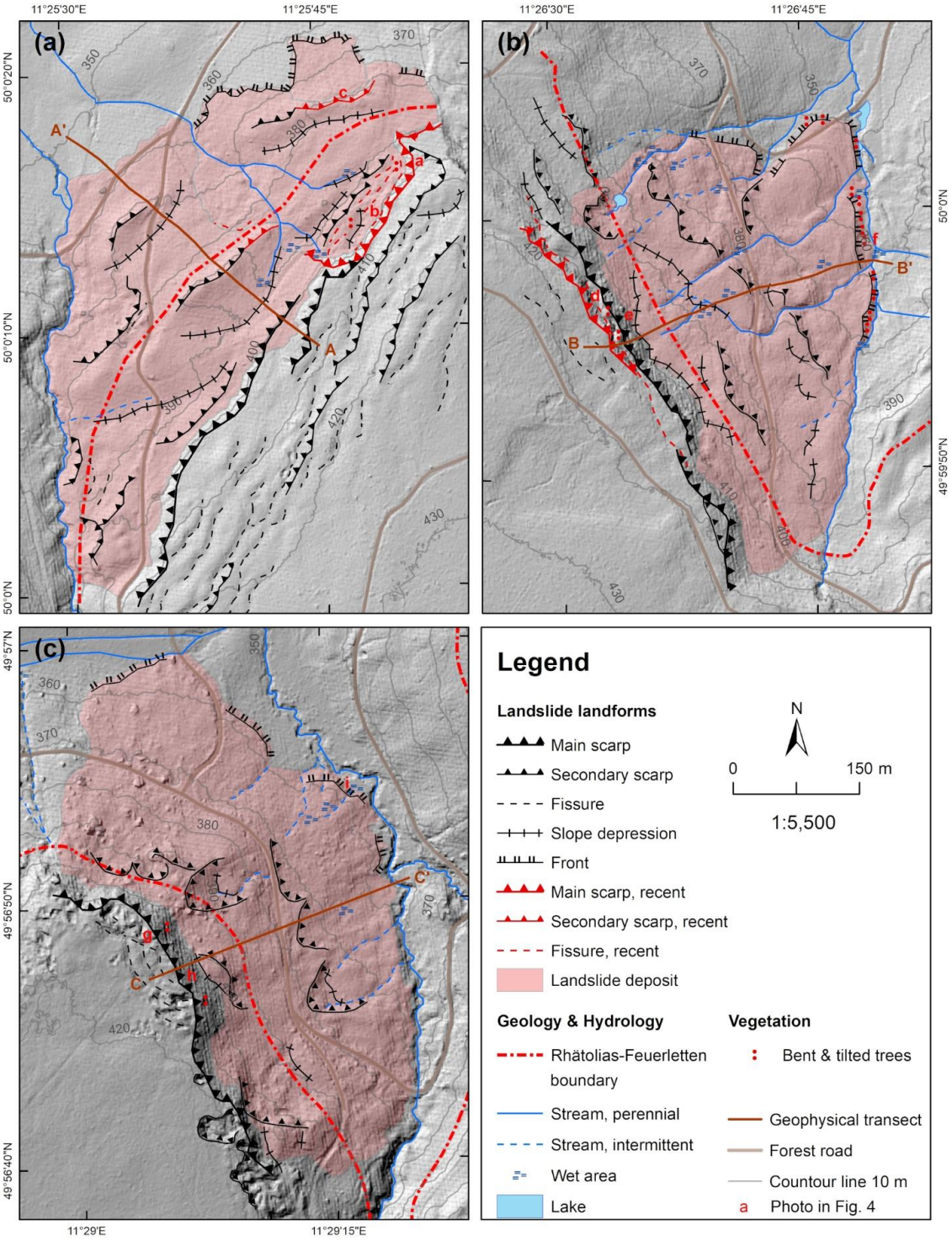

Figure 3: Geomorphic maps of the landslides at (a) Putzenstein, (b) Weinreichsgrab and (c) Fürstenanger (DEM source: Bayerische Vermessungsverwaltung). For location of landslides within the research area see Fig. 2b.

Figure 4: Photos of (a-b) lateral roots under tension located at the headscarp and (c) at a secondary scarp of the Putzenstein landslide. (d) Rhätolias boulders at the headscarp, (e) overview of the headscarp and (f) tilted trees at the toe of the Weinreichsgrab landslide. (g-h) Overview about the headscarp and (i) the toe of the Fürstenanger landslide.

4.2 Landslide thickness

The Putzenstein landslide was characterized by three high resistivity cells located at transect lengths between 5 and 70 m, 70 to 195 m and 232 to 315 m with resistivities up to 4,000 Ohm m (Fig. 5a). The cells' thickness ranged from 18 m at the

beginning of the transect to 7 m at the lower part of the transect. The underlying areas below these cells had low and contrasting resistivities that enabled a clear differentiation from the near surface areas (Fig. 5a and S3a-c). Between the high-resistivity cells, the ERT revealed two low-resistivity bodies between 195 and 220 m as well as between 315 and 330 m transect length with low contrast to underlying areas (Fig. S3d). The Weinreichsgrab landslide was characterized by high-resistivity areas near the surface until transect length 320 m (Fig. 5b) with underlying low-resistivity areas from 9 m depth on (Fig. S3e-g). The high-resistivity areas were differentiated into three cells in clear contrast to underlying low-resistivity areas, while the lower part of the transect from 320 m on showed low resistivities between 20 and 70 Ohm m with low contrast to underlying areas (Fig. S3h). The Fürstenanger landslide revealed heterogeneous near surface conditions with alternating high-resistivity and low-resistivity areas (Fig. 5c). At transect length 50 to 110 m, an up to 15 m thick high resistivity body was located. From 110 m on, the transect was characterized by alternating low- and high resisting cells and a more or less consistent zone of contrasting resistivities at 4 m depth (Fig. S3j, l). This pattern was disturbed at 180 m transect length, where areas of higher resistivities dipped 45° into the slope resulting in a 10-12 m thick zone of contrasting low and high resistivities (Fig. S3k).

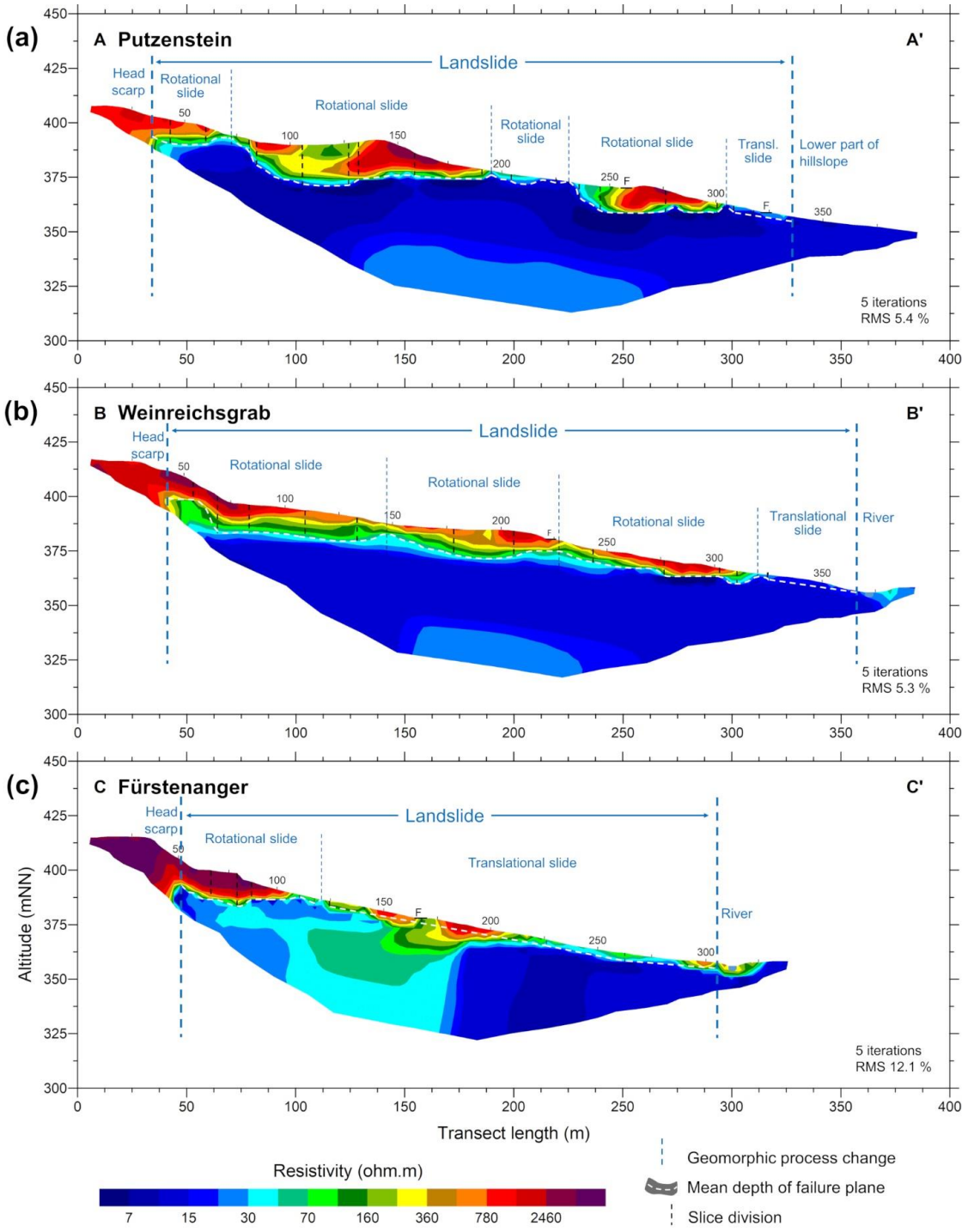

Figure 5: Geoelectric models and landslide forms at (a) Putzenstein, (b) Weinreichsgrab and (c) Fürstenanger. Failure plane depth was derived from vertical resistivity decrease in order of one to two magnitudes. For detailed derivation, see Figure S3 in the Supplementary Information. F highlights location of forest roads

4.3 Trees and roots

The tree mapping results on all transects showed high spatial variability of tree species composition. The Putzenstein landslide showed a clearing with seedlings of different species including Scots pine, European silver fir and European larch above the headscarp and until transect length 75 m (Fig. 6a). From 75 m on, the tree cover got denser with young Norway spruces and European beeches. Between 180 m and 235 m transect length, the trees were characterized by young Norway spruces and European beeches of mixed ages. Norway spruces became dominant from 235 m on and grew in form of a dense thicket between the first forest road at 260 m and the second forest road at 325 m. Below the second forest road, an abrupt change occurred and trees were characterized by Norway spruces, European beeches and Scots pines of different ages. Above the headscarp of the Weinreichsgrab landslide (Fig. 6b), old trees stood in an open high forest, mixed with the grouped regeneration of Norway spruce. Between 40 and 150 m transect length, young European beeches and European silver firs grew with Scots pines that added to the regeneration. From 150 m on, the species mixed with older Norway spruce trees until the forest road at 225 m. Below the forest road, Norway spruces were dominant and young Norway spruces grew in thickets. From 320 m on, many Norway spruces and few European beeches occurred, but were misaligned or dead. The area above the headscarp of the Fürstenanger landslide and from transect length 50 to 120 m was characterized by Scot pines (Fig. 6c). From transect length 120 m on, Norway spruce became the dominant species and grew in form of a thicket from 150 m until the forest road at 170 m. Below the forest road, Norway spruces with a few European beeches and Scots Pines occurred until 280 m transect length, while Norway spruces were dominant at the landslide toe.

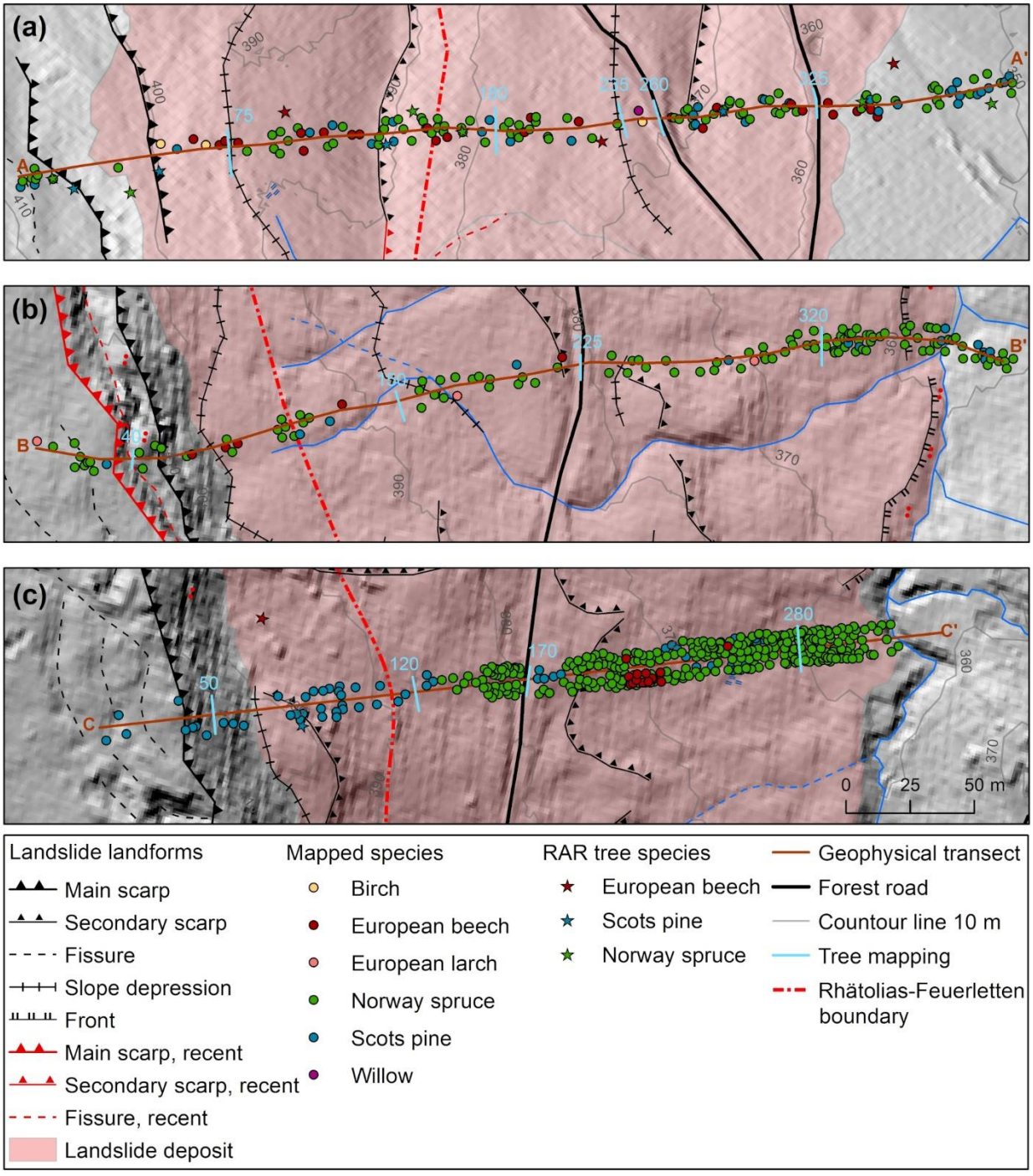

Figure 6: Mapped trees with height above 4 m in up to 5 m distance to the ERT transects (Fig. 5) at (a) Putzenstein, (b) Weinreichsgrab and (c) Fürstenanger. The locations of ERT transects are shown in Fig. 3.

From 160 root tensile strength tests, 27 tests showed a root breakage in the middle and were used to develop a tensile strength root diameter relationship (Fig. 7). This relationship is characterized by an exponential decrease of tensile strength with increasing root diameter (14.22 $d^{-1.13}$, r^2=0.55; Fig. 6). Roots were restricted to the upper 0.5 m for Scots pines and Norway spruces and to 0.4 m for European beeches. The RAR showed no differences between Rhätolias or Feuerletten. For Norway spruce, mean root area ratio decreased from the surface to 0.5 m with values between 0.19 and 0.2 % at 0 to 0.2 m depth, 0.04 % at 0.2 to 0.4 m depth and 0.005 % between 0.4 and 0.5 m depth (Fig. 8a). Only the depth between 0.1 and 0.2 m showed a variation between the sites. Scots pines showed a similar RAR trend with RAR values between 0.16 and 0.19 % between 0 and 0.2 m, 0.01% between 0.2 and 0.3 m, 0.04 % and 0.11% between 0.3 and 0.5 m depth (Fig. 8b). The variability was highest from 0 to 0.3 m depth between measurement locations. European beeches revealed a similar RAR depth pattern, however, with increased magnitudes and variability. Mean RAR decreased from 0.42 % between 0 and 0.1 m depth to 0.15 and 0.12 % between 0.1 and 0.4 m depth (Fig. 8c). Root cohesion revealed similar depth patterns as RAR. For Norway spruce, mean root cohesion showed 12 to 12.4 kPa for 0 to 0.2 m depth and decreased to 3.6 kPa between 0.2 and 0.3 m, 2.6 kPa between 0.3 and 0.4 m and 0.7 kPa between 0.4 and 0.5 m depth (Fig. 8d). Scots pine revealed lower root cohesion. Mean root cohesion increased from 4.3 kPa between 0 and 0.1 m to 6 kPa between 0.1 and 0.2 m depth (Fig. 8e). With increasing depth, mean root cohesion fluctuated between 1.6 and 2.3 kPa. European beeches showed the highest root cohesion magnitude and variability. Mean root cohesion decreased from 23.6 kPa for the upper 0.1 m to a range between 8.4 and 12.5 kPa for depths between 0.1 and 0.4 m (Fig. 8f).

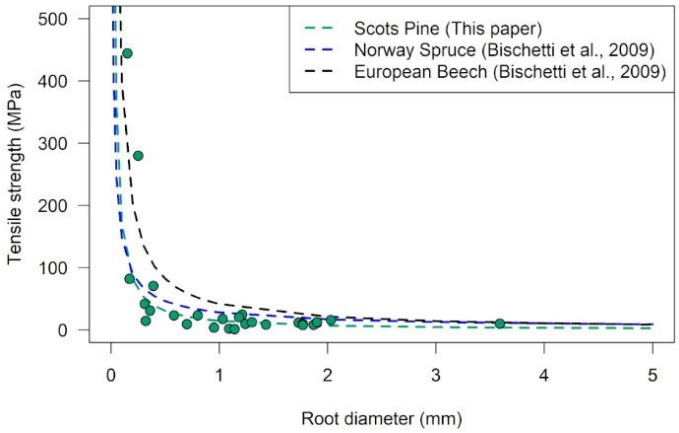

Figure 7: Tensile strength plotted versus root diameter for Scots pine compared to power laws derived for European beech and Norway spruce.

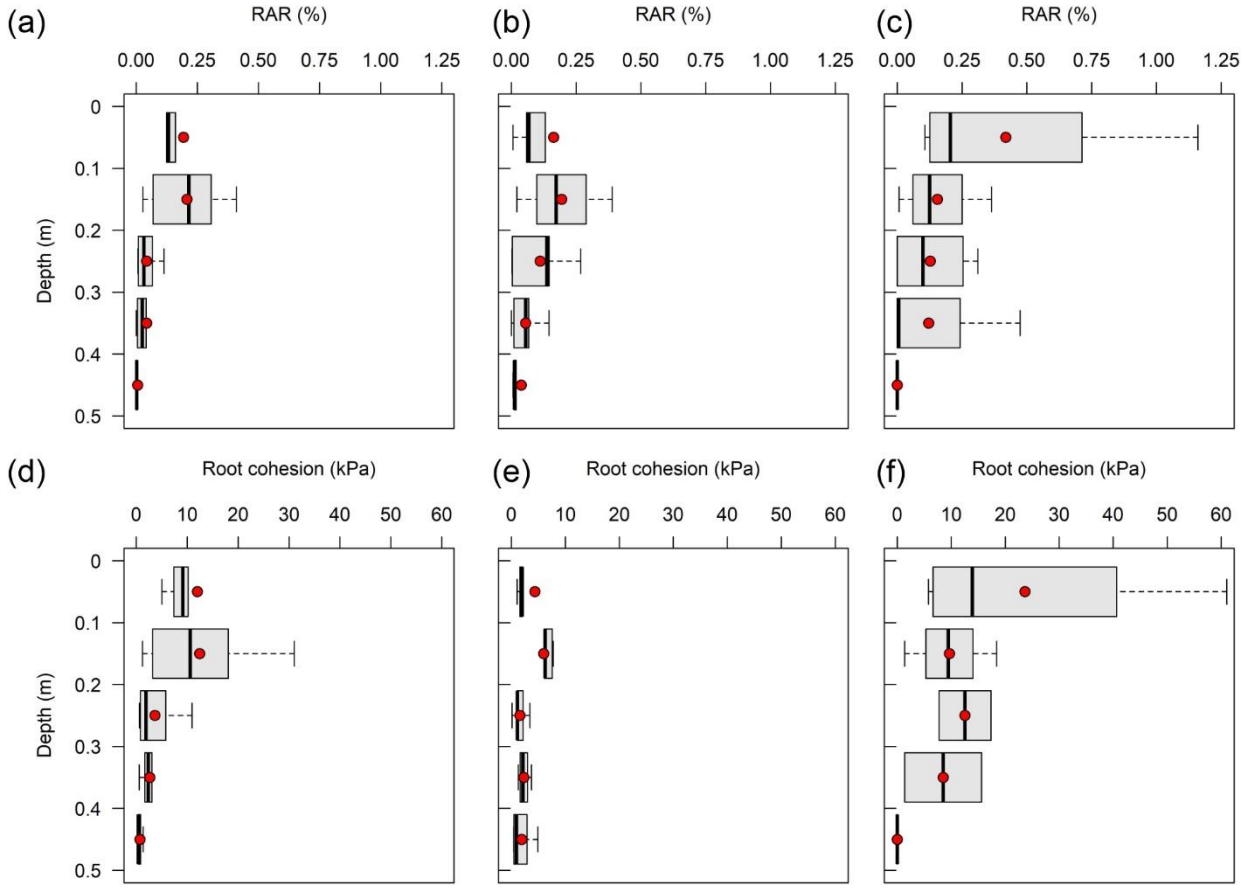

Figure 8: Root area ratio plotted against depth for (a) Norway spruce, (b) Scots pine and (c) European beech. Root cohesion plotted against depth for (d) Norway spruce, (e) Scots pine and (f) European beech. Red dots highlight mean RAR or root cohesion.

330

4.4 Landslide stability analysis

4.4.1 Landslide stability scenarios for deep-seated landslides

All three landslides revealed shear planes far below rooting depth and showed stable conditions with factor of safety (FoS) values above 1.66 when assuming a soil cohesion of 28.6 kPa (Fig. 9). Assuming a residual cohesion of 8.5 kPa resulted in
335 FoS values all over 1 at all water levels at Putzenstein landslide (Fig. 9a). For Weinreichsgrab and Fürstenanger landslides, stability depended on the slice height scenario. The Weinreichsgrab landslide became instable when saturation increases above 0.8 in the upper slice height scenario (Fig. 9b). The Fürstenanger landslide undercut a factor of safety of 1 at full saturation for the mean and at 0.8 for the upper slice height scenario (Fig. 9c). Assuming no residual soil cohesion, the Fürstenanger landslide would be instable independent of saturation levels (Fig. 9c). The Putzenstein landslide would become instable between a
340 saturation level of 0.65 and 1.0 depending on shear plane scenario (Fig. 9a). The Weinreichsgrab landslide would be instable for maximum shear plane scenario independent of saturation and for mean and minimum shear plane scenario above 0.55

(Fig. 9b). Assuming, full saturation would reduce soil cohesion to zero, all scenarios for all landslides would show a FoS below 1.

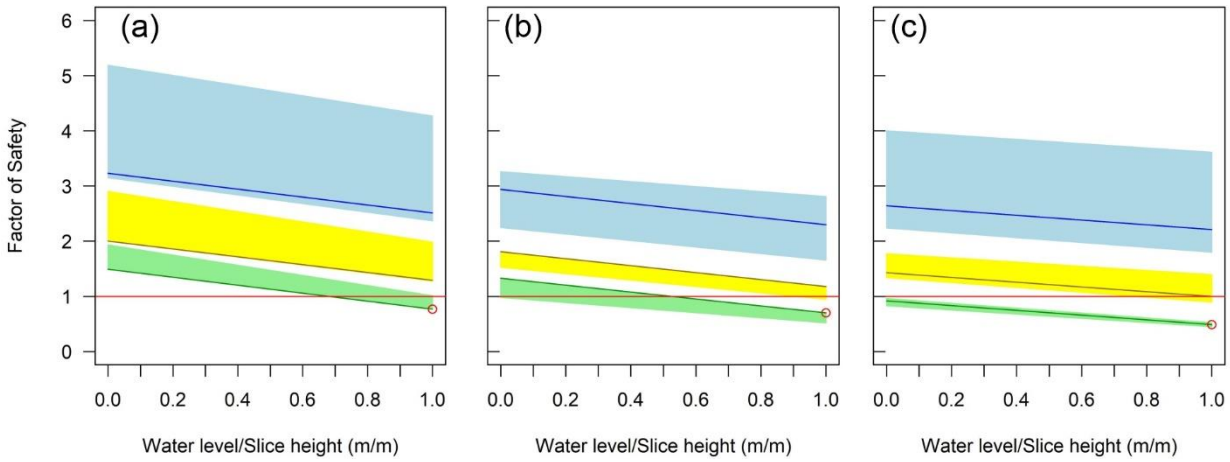

Figure 9: Factor of safety models for the reactivation of the landslides at (a) Putzenstein, (b) Weinreichsgrab, and (c) Fürstenanger. We assume an angle of internal friction of 8.4°. We vary cohesion between 28.6 kPa (blue scenario), 8.5 kPa (yellow) and 0 kPa (green). Calculations are based on a mean shear plane depth (line) and minimum and maximum shear plane depth (rectangle).

4.4.2 Stability scenarios for shallow landslides above road cuts and landslide toes

Root cohesion can act as basal root cohesion when penetrating the shear plane and as lateral root cohesion when anchoring the soil during scarp development. We calculated which minimum combined soil and root cohesion is necessary to prevent the occurrence of shallow translational landslides above road cuts and at landslide toes. All these locations are underlain by Feuerletten and assuming a soil cohesion of 28.6 kPa or a residual soil cohesion of 8.5 kPa would result in stable conditions (Fig. 10). When the soil is oversaturated, soil cohesion can be zero. In this case, a minimum root cohesion between 0.8 kPa for shear planes at 0.3 m and 4.5 kPa for shear planes at 1.5 m would be sufficient to stabilize the soil above road cuts (Fig. 10a). At landside toes, root cohesion between 0.25 and 0.8 kPa are required to stabilize a potential landslide with a shear plane at 0.3 m depth and root cohesion between 0.9 and 3.6 kPa to stabilize landslides with shear planes of 1.5 m depth (Fig. 10b).

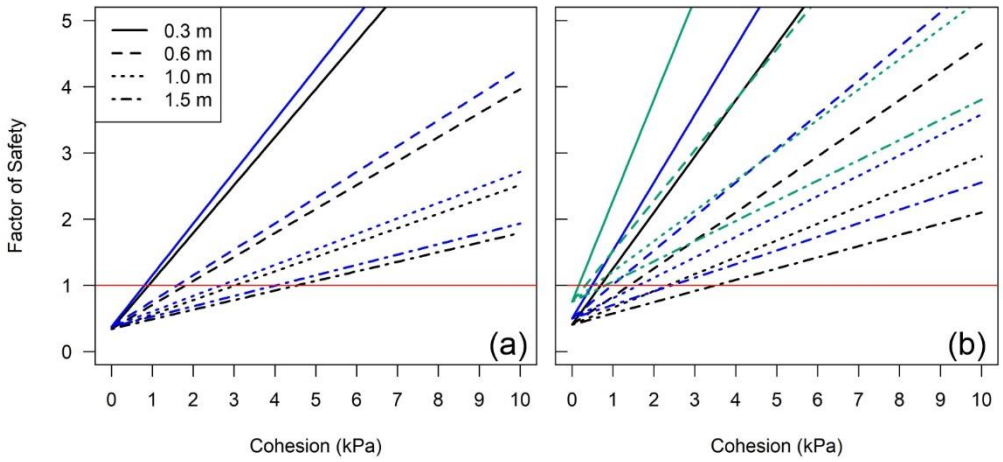

Figure 10: Factor of safety for full-saturated conditions with a residual angle of friction of 8.4° plotted against cohesion scenarios ranging from no cohesion to 10 kPa for (a) translational landslides at road cuts and (b) landslide toes. Line style highlight the depth of shear plane ranging between 0.3 m and 1.5 m. Line colour in (a) refer to Putzenstein (black) with a slope angle of 13°, Weinreichsgrab and Fürstenanger (both blue) with slope angles of 12°. Line colour in (b) refer to Putzenstein (black) with a slope angle of 11°, Weinreichsgrab (blue) with a slope angle of 9° and Fürstenanger (green) with a slope angle of 6°.

5 Discussion

5.1 Geologic control on deep-seated landsliding

The combination of high-permeable Rhätolias above Feuerletten controls deep-seated landsliding. Of the 125 observed landslides in our research area, 95 % occurred at the Rhätolias-Feuerletten boundary (Fig. 2b), which suggests that Feuerletten play a key role in landsliding. The Feuerletten possess a lower angle of internal friction than Rhätolias (Table 1) and cohesion of these clays is susceptible to saturation. Previous landslide inventories of the Franconian Alb support this role of Feuerletten in the North-Bavarian scarplands, where Feuerletten were responsible for an inappropriate high proportion of landslides (Kany and Hammer, 1985). Kany and Hammer (1985) assumed that most landslides were fossil and occurred under past climatic conditions, however, they suggested that these deep-seated landslides could be reactivated due to anthropogenic impacts as road cutting and forestry. The observed movement of the Thurnau landslide affecting the highway (Fig. 2b; Wilfing et al., 2018) supports the argument of potential reactivation.

The ERT enabled the identification of the shear plane location and suggested that landslides are complex with rotational and translational movement. The Putzenstein landslide revealed a hummocky topography (Fig. 3a) and the ERT showed three high-resistivity cells with resistivities up to 4,000 Ohm m and a thickness between 7 and 18 m located above low-resistivity bodies at transect length between 5 and 70 m, 70 to 195 m and 232 to 315 m (Fig. 5a). Pürckhauer drillings revealed fine and silty sand in the upper 1 m. We interpret these cells as dry Rhätolias above wet Feuerletten. The form of these cells and the hummocky topography indicate three rotational slabs. In between the lower high-resistivity cells, low resistivities indicate a water-saturated rotational slab (Fig. 5a). The lower part of the landslide was characterized by a flat topography, low-resistivity areas, and near-surface clay material. Therefore, we interpret this landslide part as a translational slide within the Feuerletten.

The Weinreichsgrab landslide revealed a similar pattern of three high-resistivity cells within hummocky terrain with near-surface silty sand followed by flat terrain with low resistivities and near-surface clay (Fig. 5b). These results indicate three rotational slabs and one translational slab at the toe of the landslide. In contrast, the Fürstenanger landslide showed one high-resistivity area in the upper part indicating a rotational failure (Fig. 5c). However, the major part of the landslide showed heterogeneous near-surface resistivities underlain by low resistivities in form of a straight slope indicating a translational landslide. The observed resistivity pattern was disturbed at 180 m transect length, where areas of higher resistivities dipped 45° into the slope resulting in a 10-12 m thick zone of contrasting low and high resistivities (Fig. S3 k). However, the topography showed no evidence of a rotational slide, therefore, we interpret the resistivity pattern as an artefact of the measurement rather than an indicator for rotational movement. In summary, electrical resistivity tomography enabled in most conditions the identification of the shear plane due to high resistivity contrasts between Rhätolias and Feuerletten with an uncertainty depending on the resolution of the tomography in the range of 2.5 m. Therefore, we established minimum, mean and maximum shear plane depth scenarios to propagate the uncertainty into our stability analysis. All shear plane scenarios showed a shear plane location far below rooting depth of trees observed on the landslides indicating that root cohesion by trees plays no role in stabilisation of deep-seated landslides.

Reactivation of deep-seated landslides depends on cohesion and water saturation. As soil cohesion showed a large variation between individual layers and within each layer of the Feuerletten (Table 1; Boley Geotechnik, 2018; Wilfing et al., 2018), we used three different cohesion scenarios in combination with the residual internal angle of friction of 8.4° measured by Boley Geotechnik (2018) for the stability analysis. Our landslide stability analysis showed that all three landslides revealed stable conditions independent of saturation with FoS values above 1.66 when assuming a soil cohesion of 28.6 kPa (Fig. 9). This high cohesion is the mean soil cohesion of soft silty Feuerletten clay (Table 1) and potentially representative for undisturbed Feuerletten. According to laboratory tests by Ikari and Kopf (2011), soil cohesion can re-develop in clays after landsliding due to normal stress. To include this scenario, we used a reduced soil cohesion of 8.6 kPa (1/3 of the original value). When assuming a residual cohesion, an FoS below 1 is not reached at Putzenstein landslide independent of water level (Fig. 9a), at Weinreichsgrab below saturation of 0.8 in the upper slice height scenario (Fig. 9b) and at Fürstenanger below 0.8 for the maximum and 1.0 for the mean shear plane scenario (Fig. 9c). The development of high saturation in the sand layers of Rhätolias is unlikely as sand is very permeable. However, Rhätolias has impermeable clay layers (Boley Geotechnik, 2018) and tectonic-induced fractures can increase water infiltration through these clay layers (Wilfing et al., 2018). Therefore, water can be trapped between clay layers in Rhätolias and clay layers in underlying Feuerletten, which can cause hydrostatic pressures equal to high saturation levels (Rogers and Selby, 1980; Selby, 1993). Therefore, a reactivation of the entire landslide could be possible due to the geologic conditions of alternating clay layers within the Rhätolias underlain by impermeable Feuerletten. Assuming no residual soil cohesion as suggested by Skempton (1985), the Fürstenanger landslide would be instable independent of saturation level and shear plane scenario (Fig. 9b-c), while the Putzenstein and Weinreichsgrab landslide would get instable between a saturation level of 0.65 to 1.0 and 0 to 0.5 depending on shear plane scenario (Fig. 9a-b). However, there are no indicators for a reactivation of the Fürstenanger landslide while recent fissures indicate potential

reactivation of Putzenstein and Weinreichsgrab landslides (Fig. 3a-b). The applied model scenarios showed a large variation of stability states depending on chosen soil cohesion and water availability. The application of landslide models incorporating hydrological conditions (e.g. Perkins et al., 2017) can improve the assessment of slope stability.

5.2 Vegetation control on shallow landsliding

Root area ratio plays a more important role in stabilisation of shallow landslides than tensile strength. Based on 27 tests, we developed a tensile strength root diameter relationship for Scots pines, which is characterized by an exponential decrease of tensile strength with increasing root diameter (r^2=0.55; Fig. 6). Therefore, relative tensile strength increases with decreasing root diameters (Stokes et al., 2009) as thinner roots possess a higher cellulose content that provides additional strength (Genet et al., 2005). The power law and the statistical degree is in the range of previous measurements on European beeches and Norway spruces (Fig. 6; Genet et al., 2005; Bischetti et al., 2009) and show only little difference between species (Genet et al., 2005; Hales, 2018). Our RAR measurements revealed two times higher RAR values for European beeches than Scots pines or Norway spruces (Fig. 8a-c). Consequently, root cohesion is much higher for European beech than Scots pine and Norway spruce (Fig. 8d-f). A decrease in tree species number of Scots pine and Norway spruce with an increase of European beech as planned by the forest management (personal communication by F. Maier) would increase the root cohesion and therefore slope stability.

Local soil conditions are controlled by geology and geologically affected soil conditions at hillslope scale reduce rooting depth (Fig. 1). Our RAR measurements showed that roots were restricted to the upper 0.5 m for Scot pines and Norway spruces and to 0.4 m for European beeches (Fig. 8a-c). Within a species, RAR revealed no differences between topographic locations at the slope or between Rhätolias or Feuerletten. The rooting depth was very low compared to pines and beeches occurring in the near-by Frankenwald that showed rooting depth up to 1.2 m (Nordmann et al., 2009), however, lithology and soil conditions are different, which seem to influence root properties more than species identity (Lwila et al., 2021). At upper slope location, Rhätolias is abundant and characterized by high permeable sandy soil (Fig. 1b). In dry soils, trees usually develop deeper roots to reach groundwater (Hoffmann and Usoltsev, 2001), however, the hard sandstone layers within the Rhätolias prevent deeper rooting (Fig. 1b). In addition, sandy soils are less deeply warmed than fine-grained soils which results in shallower root growth (Kutschera and Lichtenegger, 2002). At lower slope locations, clayey Feuerletten are abundant (Fig. 1c) which resulted in combination with slope-induced water flow in moist conditions. Moist aerated soils are characterized by extreme flat rooting (Stone and Kalisz, 1991; Kutschera and Lichtenegger, 2002). Therefore, lithology and associated soil conditions in combination with topography-controlled water flow resulted in low rooting depth. Consequently, basal root cohesion can only effect shallow landslides with a shear plane below 0.4 or 0.5 m depth, respectively.

Tree density plays an important role in shallow landslide stabilisation by controlling lateral root cohesion. Tensed roots at Putzenstein (Fig. 4a-c) and bent or tilted trees at Weinreichsgrab (Fig. 4f) indicate soil creep or shallow landsliding in the upper 1 to 1.5 m of Feuerletten clay (Fig. 3a-b). To quantify the minimum root cohesion necessary to stabilise low-inclined

slopes, we tested shallow landsliding with shear planes up to 1.5 m depth for slopes affected by forest road cuts and at landslide toes with clay material near the surface enabling high saturation (m=1). Slopes above forest road cuts were characterized by low inclination between 11 and 12°, while landslide toes revealed even lower slope angles in the range of 6 to 9°. Assuming a shear plane depth of 0.3 m, slopes above road cuts and landslide toes would require a cohesion between 0.2 and 0.8 kPa (Fig. 10) to stabilize the slope. As root cohesion of Norway spruce, Scots pine and European beech between 0.3 and 0.4 m depth is above 1 kPa (Fig. 8d-f), root cohesion would be sufficient to stabilize the slope. However, species distribution, number and position have an influence on the occurrence of landslides (Roering et al., 2003), as the vegetation patterns always leave gaps with lower root cohesion. Our investigated slopes above road cuts were characterized by a combination of European beech and Norway spruce at Putzenstein and Weinreichsgrab landslides (Fig. 6a-b), which grew dense enough to provide sufficient root cohesion to stabilize the slopes. Dense thickets of Norway spruce occurred on Fürstenanger slopes above road cuts and on all landslide toes (Fig. 6c) and provide high root density that would enable sufficient stabilization. When shear planes exceed rooting depth, lateral root cohesion can have a stabilizing effect (Schwarz et al., 2010b) by affecting the onset and size of shallow landsliding (Schmidt et al., 2001; Roering et al., 2003) as indicated by tensed roots observed at Putzenstein (Fig. 4b). To stabilize shallow landslides with shear planes up to 1.5 m, our calculations showed that a cohesion between 1 and 4.5 kPa would be required (Fig. 10). As lateral root cohesion is the sum of root cohesion of rooted depth, all three investigated species would provide sufficient lateral root cohesion to stabilize the slope (Fig. 8d-f) independent of potential soil cohesion, when spacing of trees enable an entire cover of the slope. Sufficient tree cover is provided at landslide toes and at the slope above the road cut at Fürstenanger (Fig. 6c), where thickets of Scots pine are abundant. Above road cuts at Putzenstein and Weinreichsgrab, European beeches occur that provide the highest calculated root cohesion (Fig. 8f). Our analysis excluded dead or harvested trees that can provide additional root cohesion until they rot away (e.g. Ammann et al., 2009; Vergani et al., 2017), therefore, we eventually underestimate both basal and lateral root cohesion. Despite the calculations suggest that lateral root cohesion should prevent shallow landsliding, tilted and bent trees especially at Weinreichsgrab (Fig. 4f) indicate the occurrence of soil creep and potential slow shallow landslide movement (Van Den Eeckhaut et al., 2009; Pawlik and Šamonil, 2018).

5.3 Potential impacts of forestry activity on future shallow landsliding

Forestry activities influence slope stability. Roots decay after forest cutting results in decreasing strength and RAR decreases (Vergani et al., 2014; Vergani et al., 2016) already relevant one year after tree cutting (Sidle and Bogaard, 2016; Zhu et al., 2020). In addition to reduction of root cohesion by timber harvesting (Vergani et al., 2016) or small-scale logging (Bischetti et al., 2016), the harvesting process can result in soil erosion (Haas et al., 2020) and the construction of new forest access roads increases instability through slope fragmentation and altered drainage (Borga et al., 2005; van Beek et al., 2008). Forestry activity can induce gaps in the forest cover that would decrease the effect of lateral root cohesion (Cohen and Schwarz, 2017). Therefore, forestry activity at slopes or above road cuts could decrease root cohesion sufficiently to trigger landslides in case of non-existing soil cohesion due to high saturation levels. Regeneration of young trees may already provide a considerable

amount of root reinforcement but takes years to restore the original root cohesion (Sidle and Ochiai, 2006; Giadrossich et al., 2020).

Climate change will result in higher probability of dry summers and wet winters (Estrella and Menzel, 2013). On dry locations as permeable Rhätolias sandstone, droughts can affect the growth of Norway spruce, Scots pine and with less effect of European beech (Debel et al., 2021). In the research area, forest management aims to adapt tree composition to climate change (Keenan, 2015). In detail, the forest service aims to reduce the number of Norway spruce and increase the percentage of European beech (personal communication by F. Maier). Our RAR and root cohesion data (Fig. 8) suggests that a species change towards European beech would increase root reinforcement on the slopes when a sufficient rooted area has been developed. Furthermore, the forestry service will diversify the tree composition by planting European sliver fir (*Abies alba*), Norway maple (*Acer platanoides*), European alder (*Alnus glutinosa*), sessile oak (*Quercus petraea* (Matt.) Liebl.), pendunculate oak (*Quercus robur* R.), Silver birch (*Betula pendula* Roth) and downy birch (*Betula pubescens* Ehrh.) and diversify tree age (personal communication by F. Maier). Previous investigations on plant diversity showed that tree mixture had no influence on FoS as root tensile strength plays a minor role in stability (Genet et al., 2010). However, root strength decreases with age (Sidle and Bogaard, 2016), therefore, a mixed age forest can prevent root strength decay as young trees can compensate the reduction of root strength of old trees. Our root cohesion data showed (Fig. 8) that lateral root cohesion is sufficient to stabilise slopes (Fig. 10), when tree distribution is dense enough to avoid gaps. Therefore, stability is more a factor of tree size and density (Genet et al., 2010), and forest management should aim to achieve a dense enough forest that provides sufficient lateral and basal root cohesion (Fig. 10) to avoid future shallow landsliding.

6 Conclusion

Scarplands are characterized by alternating sedimentary layers with different strength properties. In our study, we observed 125 deep-seated landslides that indicate a geologic control on landsliding by impermeable Feuerletten underlying more permeable Rhätolias. Detailed investigations on three landslides showed that shear planes occurred at depth to deep for tree roots, therefore, roots play no role for stabilization of deep-seated landslides. The wide range of potential material strength properties result in high uncertainty of landslide stability analysis. Scenarios incorporating original soil cohesion showed stable conditions independent of saturation while cohesion-less scenarios indicated unstable scenarios independent or starting at low saturation levels. Mean soil cohesion scenarios revealed unstable conditions limited to high saturation levels. These saturation levels seem to be unlikely, however, unfavourable geologic conditions could result in high water pressures that develop between impermeable Feuerletten and clay layers within Rhätolias, reactivating deep-seated landslides.

Vegetation control is restricted to shallow landsliding. Roots of trees are limited to the upper 0.5 m due to unfavourable dry conditions at Rhätolias locations or unfavourable wet conditions, where Feuerletten are abundant. Root tensile strength is comparable between Norway spruce, Scots pine and European beech and root cohesion is mainly controlled by root area ratio. Therefore, shallow landsliding is highly unlikely at near-surface depth (0.3 m) where basal root cohesion provides sufficient

stability. Below 0.5 m, lateral root cohesion can stabilize slopes even under high saturation without soil cohesion if gaps between trees are avoided. Forest management can reduce landslide susceptibility by providing sufficient tree density and avoiding large scale harvesting.

7 Data availability

The DEM can be bought from Bayerisches Landesamt für Digitalisierung, Breitband und Vermessung (https://www.ldbv.bayern.de/produkte/3dprodukte/gelaende.html). The landslide inventory of Bavaria can be downloaded from the Bayerisches Landesamt für Umwelt (https://www.lfu.bayern.de/umweltdaten/geodatendienste/pretty_downloaddienst.htm?dld=georisiken). All data produced by the authors in this study is available at figshare (https://doi.org/10.6084/m9.figshare.20368464.v1).

8 Author contribution: DD designed the study and wrote the manuscript with contributions of TG and MP. All authors collected the ERT data. TG mapped the landslides and processed the ERT data as part of his BSc thesis. MP mapped tree location, measured tensile strength and root area ratios as part of her MSc thesis. DD re-analysed the landslide stability based on the theses by TG and MP.

9 Competing interests: The authors declare no competing interest.

10 Acknowledgements

The authors thank Fritz Maier and his team at Bayerische Staatsforsten Nordhalben for their support.

References

Ad-hoc-AG Boden: Bodenkundliche Kartieranleitung, 5th ed., Schweizerbart'sche, Stuttgart, 2005.

Ammann, M., Böll, A., Rickli, C., Speck, T., and Holdenrieder, O.: Significance of tree root decomposition for shallow landslides, Forest Snow and Landscape Research, 82, 79, 2009.

Bayerisches Geologisches Landesamt: Geological Map of Bavaria 1:25.000, Nr. 6034 Mistelgau, München, 1955.

Bayerisches Geologisches Landesamt: Geological Map of Bavaria 1:25.000, Nr. 6035 Bayreuth, München, 1977.

Bayerisches Geologisches Landesamt: Preliminary of Geological Map of Bavaria 1:25.000, Nr. 5934 Thurnau, München, not yet published.

Bischetti, G. B., Chiaradia, E. A., Epis, T., and Morlotti, E.: Root cohesion of forest species in the Italian Alps, Plant Soil, 324, 71-89, https://doi.org/10.1007/s11104-009-9941-0, 2009.

Bischetti, G. B., Bassanelli, C., Chiaradia, E. A., Minotta, G., and Vergani, C.: The effect of gap openings on soil reinforcement in two conifer stands in northern Italy, Forest Ecology and Management, 359, 286-299, https://doi.org/10.1016/j.foreco.2015.10.014, 2016.

Boley Geotechnik: Trassenverschiebung aus Rutschhangbereich bei Thurnau. Geotechnischer Bericht zum Feststellungsentwurf. Report, München, 2018.

Borga, M., Tonelli, F., Fontana, G. d., and Cazorzi, F.: Evaluating the influence of forest roads on shallow landsliding, Ecological Modelling, 187, 85-98, https://doi.org/10.1016/j.ecolmodel.2005.01.055, 2005.
Bromhead, E. N.: Reflections on the residual strength of clay soils, with special reference to bedding-controlled landslides, Quarterly Journal of Engineering Geology and Hydrogeology, 46, 132-155, https://doi.org/10.1144/qjegh2012-078, 2013.
Chambers, J. E., Wilkinson, P. B., Kuras, O., Ford, J. R., Gunn, D. A., Meldrum, P. I., Pennington, C. V. L., Weller, A. L., Hobbs, P. R. N., and Ogilvy, R. D.: Three-dimensional geophysical anatomy of an active landslide in Lias Group mudrocks, Cleveland Basin, UK, Geomorphology, 125, 472-484, https://doi.org/10.1016/j.geomorph.2010.09.017, 2011.
Chandler, R. J.: Clay Sediments in Depositional Basins: the Geotechnical Cycle, Quarterly Journal of Engineering Geology and Hydrogeology, 33, 7-39, https://doi.org/10.1144/qjegh.33.1.7, 2000.
Cohen, D., and Schwarz, M.: Tree-root control of shallow landslides, Earth Surface Dynamics, 5, 451-477, https://doi.org/10.5194/esurf-5-451-2017, 2017.
Crozier, M. J.: Deciphering the effect of climate change on landslide activity: A review, Geomorphology, 124, 260-267, https://doi.org/10.1016/j.geomorph.2010.04.009, 2010.
Debel, A., Meier, W. J.-H., and Bräuning, A.: Climate Signals for Growth Variations of F. sylvatica, P. abies, and P. sylvestris in Southeast Germany over the Past 50 Years, Forests, 12, 1433, https://doi.org/10.3390/f12111433, 2021.
Deljouei, A., Abdi, E., Schwarz, M., Majnounian, B., Sohrabi, H., and Dumroese, R. K.: Mechanical Characteristics of the Fine Roots of Two Broadleaved Tree Species from the Temperate Caspian Hyrcanian Ecoregion, Forests, 11, 345, https://doi.org/10.3390/f11030345, 2020.
Dorren, L. K. A., Berger, F., le Hir, C., Mermin, E., and Tardif, P.: Mechanisms, effects and management implications of rockfall in forests, Forest Ecology and Management, 215, 183-195, https://doi.org/10.1016/j.foreco.2005.05.012, 2005.
Duszyński, F., Migoń, P., and Strzelecki, M. C.: Escarpment retreat in sedimentary tablelands and cuesta landscapes – Landforms, mechanisms and patterns, Earth-Sci. Rev., 196, 102890, https://doi.org/10.1016/j.earscirev.2019.102890, 2019.
Emmert, U.: Geologische Karte von Bayern 1 : 25000, Erläuterungen zum Blatt Nr. 6035 Bayreuth, Bayerisches Geologisches Landesamt, München, 1977.
Estrella, N., and Menzel, A.: Recent and future climate extremes arising from changes to the bivariate distribution of temperature and precipitation in Bavaria, Germany, International Journal of Climatology, 33, 1687-1695, https://doi.org/10.1002/joc.3542, 2013.
Fellenius, W.: Calculation of stability of earth dam, Transactions. 2nd Congress Large Dams, Washington, DC, 1936, 445-462, 1936.
Genet, M., Stokes, A., Salin, F., Mickovski, S. B., Fourcaud, T., Dumail, J.-F., and van Beek, R.: The Influence of Cellulose Content on Tensile Strength in Tree Roots, Plant Soil, 278, 1-9, https://doi.org/10.1007/s11104-005-8768-6, 2005.
Genet, M., Kokutse, N., Stokes, A., Fourcaud, T., Cai, X., Ji, J., and Mickovski, S.: Root reinforcement in plantations of Cryptomeria japonica D. Don: effect of tree age and stand structure on slope stability, Forest Ecology and Management, 256, 1517-1526, https://doi.org/10.1016/j.foreco.2008.05.050, 2008.
Genet, M., Stokes, A., Fourcaud, T., and Norris, J. E.: The influence of plant diversity on slope stability in a moist evergreen deciduous forest, Ecological Engineering, 36, 265-275, https://doi.org/10.1016/j.ecoleng.2009.05.018, 2010.
Giadrossich, F., Schwarz, M., Marden, M., Marrosu, R., and Phillips, C.: Minimum representative root distribution sampling for calculating slope stability in Pinus radiata D. Don plantations in New Zealand, New Zealand Journal of Forestry Science, 50, 5, https://doi.org/10.33494/nzjfs502020x68x, 2020.
Glade, R. C., Anderson, R. S., and Tucker, G. E.: Block-controlled hillslope form and persistence of topography in rocky landscapes, Geology, 45, 311-314, https://doi.org/10.1130/g38665.1, 2017.
Haas, J., Schack-Kirchner, H., and Lang, F.: Modeling soil erosion after mechanized logging operations on steep terrain in the Northern Black Forest, Germany, European Journal of Forest Research, 139, 549-565, https://doi.org/10.1007/s10342-020-01269-5, 2020.
Hales, T. C., Cole-Hawthorne, C., Lovell, L., and Evans, S. L.: Assessing the accuracy of simple field based root strength measurements, Plant Soil, 372, 553-565, https://doi.org/10.1007/s11104-013-1765-2, 2013.
Hales, T. C., and Miniat, C. F.: Soil moisture causes dynamic adjustments to root reinforcement that reduce slope stability, Earth Surface Processes and Landforms, 42, 803-813, https://doi.org/10.1002/esp.4039, 2017.
Hales, T. C.: Modelling biome-scale root reinforcement and slope stability, Earth Surface Processes and Landforms, 0, https://doi.org/10.1002/esp.4381, 2018.

Hoffmann, C. W., and Usoltsev, V. A.: Modelling root biomass distribution in Pinus sylvestris forests of the Turgai Depression of Kazakhstan, Forest Ecology and Management, 149, 103-114, https://doi.org/10.1016/S0378-1127(00)00548-X, 2001.
Hutchinson, J. N.: Theme lecture: Periglacial and slope processes, Geological Society, London, Engineering Geology Special Publications, 7, 283-331, https://doi.org/10.1144/gsl.Eng.1991.007.01.27, 1991.
Ikari, M. J., and Kopf, A. J.: Cohesive strength of clay-rich sediment, Geophysical Research Letters, 38, https://doi.org/10.1029/2011GL047918, 2011.
Jäger, D., Sandmeier, C., Schwindt, D., and Terhorst, B.: Geomorphological and geophysical analyses in a landslide area near Ebermannstadt, Northern Bavaria, E&G Quaternary Sci. J., 62, 150-161, https://doi.org/10.3285/eg.62.2.06, 2013.
Ji, J., Kokutse, N., Genet, M., Fourcaud, T., and Zhang, Z.: Effect of spatial variation of tree root characteristics on slope stability. A case study on Black Locust (Robinia pseudoacacia) and Arborvitae (Platycladus orientalis) stands on the Loess Plateau, China, Catena, 92, 139-154, https://doi.org/10.1016/j.catena.2011.12.008, 2012.
Kany, M., and Hammer, H.: Statistische Untersuchungen von Rutschungen im nordbayerischen Deckgebirge, in: Ingenieurgeologische Probleme im Grenzbereich zwischen Locker-und Festgesteinen, Springer, 256-265, 1985.
Keenan, R. J.: Climate change impacts and adaptation in forest management: a review, Annals of Forest Science, 72, 145-167, https://doi.org/10.1007/s13595-014-0446-5, 2015.
Kutschera, L., and Lichtenegger, E.: Wurzelatlas mitteleuropäischer Waldbäume und Sträucher, 2nd ed., Leopold Stocker Verlag, Graz, 2002.
Lapenna, V., Lorenzo, P., Perrone, A., Piscitelli, S., Rizzo, E., and Sdao, F.: 2D electrical resistivity imaging of some complex landslides in the Lucanian Apennine chain, southern Italy, Geophysics, 70, B11-B18, https://doi.org/10.1190/1.1926571, 2005.
Loke, M., and Barker, R.: Least-squares deconvolution of apparent resistivity pseudosections, Geophysics, 60, 1682-1690, https://doi.org/10.1190/1.1443900, 1995.
Lwila, A. S., Mund, M., Ammer, C., and Glatthorn, J.: Site conditions more than species identity drive fine root biomass, morphology and spatial distribution in temperate pure and mixed forests, Forest Ecology and Management, 499, 119581, https://doi.org/10.1016/j.foreco.2021.119581, 2021.
McColl, S. T.: Chapter 2 - Landslide causes and triggers, in: Landslide Hazards, Risks, and Disasters (Second Edition), edited by: Davies, T., Rosser, N., and Shroder, J. F., Elsevier, 13-41, https://doi.org/https://doi.org/10.1016/B978-0-12-818464-6.00011-1, 2022.
Meyer, K. F., and Schmidt-Kaler, H.: Jura, in: Erläuterungen zur Geologischen Karte von Bayern 1 : 500 000, Fourth edition ed., edited by: Landesamt, B. G., Bayerisches Geologisches Landesamt, München, 90-111, 1996.
Nordmann, B., Göttlein, A., and Binder, F.: Einfluss unterschiedlicher Waldbestockung auf die Abflussbildung–ein Beispiel aus einem Wassereinzugsgebiet im Frankenwald, Hydrologie und Wasserbewirtschaftung, 53, 80-95, 2009.
Pain, C. F.: Scarp retreat and slope development near picton, New South Wales, Australia, CATENA, 13, 227-239, https://doi.org/10.1016/S0341-8162(86)80015-7, 1986.
Pawlik, Ł., and Šamonil, P.: Soil creep: The driving factors, evidence and significance for biogeomorphic and pedogenic domains and systems – A critical literature review, Earth-Sci. Rev., 178, 257-278, https://doi.org/10.1016/j.earscirev.2018.01.008, 2018.
Perkins, J. P., Reid, M. E., and Schmidt, K. M.: Control of landslide volume and hazard by glacial stratigraphic architecture, northwest Washington State, USA, Geology, 45, 1139-1142, https://doi.org/10.1130/g39691.1, 2017.
Perrone, A., Lapenna, V., and Piscitelli, S.: Electrical resistivity tomography technique for landslide investigation: A review, Earth-Sci. Rev., 135, 65-82, https://doi.org/10.1016/j.earscirev.2014.04.002, 2014.
Peterek, A., and Schröder, B.: Geomorphologic evolution of the cuesta landscapes around the northern Franconian Alb - review and synthesis, Zeitschrift für Geomorphologie, 54, 305-345, https://doi.org/10.1127/0372-8854/2010/0054-0037, 2010.
Phillips, C., Hales, T., Smith, H., and Basher, L.: Shallow landslides and vegetation at the catchment scale: A perspective, Ecological Engineering, 173, 106436, https://doi.org/10.1016/j.ecoleng.2021.106436, 2021.
Roering, J. J., Schmidt, K. M., Stock, J. D., Dietrich, W. E., and Montgomery, D. R.: Shallow landsliding, root reinforcement, and the spatial distribution of trees in the Oregon Coast Range, Canadian Geotechnical Journal, 40, 237-253, https://doi.org/10.1139/t02-113, 2003.
Rogers, N. W., and Selby, M. J.: Mechanisms of Shallow Translational Landsliding during Summer Rainstorms: North Island, New Zealand, Geografiska Annaler. Series A, Physical Geography, 62, 11-21, https://doi.org/10.2307/520448, 1980.

Schmidt, K.-H., and Beyer, I.: High-magnitude landslide events on a limestone-scarp in central Germany: morphometric characteristics and climatic controls, Geomorphology, 49, 323-342, https://doi.org/10.1016/S0169-555X(02)00193-9, 2003.
Schmidt, K. M., Roering, J. J., Stock, J. D., Dietrich, W. E., Montgomery, D. R., and Schaub, T.: The variability of root cohesion as an influence on shallow landslide susceptibility in the Oregon Coast Range, Canadian Geotechnical Journal, 38, 995-1024, https://doi.org/10.1139/t01-031, 2001.
Schwarz, M., Lehmann, P., and Or, D.: Quantifying lateral root reinforcement in steep slopes – from a bundle of roots to tree stands, Earth Surface Processes and Landforms, 35, 354-367, https://doi.org/10.1002/esp.1927, 2010a.
Schwarz, M., Preti, F., Giadrossich, F., Lehmann, P., and Or, D.: Quantifying the role of vegetation in slope stability: A case study in Tuscany (Italy), Ecological Engineering, 36, 285-291, https://doi.org/10.1016/j.ecoleng.2009.06.014, 2010b.
Seidl, R., Thom, D., Kautz, M., Martin-Benito, D., Peltoniemi, M., Vacchiano, G., Wild, J., Ascoli, D., Petr, M., Honkaniemi, J., Lexer, M. J., Trotsiuk, V., Mairota, P., Svoboda, M., Fabrika, M., Nagel, T. A., and Reyer, C. P. O.: Forest disturbances under climate change, Nature Climate Change, 7, 395-402, https://doi.org/10.1038/nclimate3303, 2017.
Selby, M. J.: Hillslope Materials and Processes, Oxford University Press, Oxford, 1993.
Sidle, R., and Ochiai, H.: Processes, prediction, and land use, Water resources monograph. American Geophysical Union, Washington, 2006.
Sidle, R. C., and Bogaard, T. A.: Dynamic earth system and ecological controls of rainfall-initiated landslides, Earth-Sci. Rev., 159, 275-291, https://doi.org/10.1016/j.earscirev.2016.05.013, 2016.
Siewert, M. B., Krautblatter, M., Christiansen, H. H., and Eckerstorfer, M.: Arctic rockwall retreat rates estimated using laboratory-calibrated ERT measurements of talus cones in Longyeardalen, Svalbard, Earth Surface Processes and Landforms, 37, 1542-1555, https://doi.org/10.1002/esp.3297, 2012.
Skempton, A., and De Lory, F.: Stability of natural slopes in London clay, Proceedings of the 4th International Conference on Soil Mechanics, 2, 378-381, 1957.
Skempton, A. W.: Long-Term Stability of Clay Slopes, Géotechnique, 14, 77-102, https://doi.org/10.1680/geot.1964.14.2.77, 1964.
Skempton, A. W.: Residual strength of clays in landslides, folded strata and the laboratory, Géotechnique, 35, 3-18, https://doi.org/10.1680/geot.1985.35.1.3, 1985.
Spreafico, M. C., Cervi, F., Francioni, M., Stead, D., and Borgatti, L.: An investigation into the development of toppling at the edge of fractured rock plateaux using a numerical modelling approach, Geomorphology, 288, 83-98, https://doi.org/10.1016/j.geomorph.2017.03.023, 2017.
Stokes, A., Atger, C., Bengough, A. G., Fourcaud, T., and Sidle, R. C.: Desirable plant root traits for protecting natural and engineered slopes against landslides, Plant Soil, 324, 1-30, https://doi.org/10.1007/s11104-009-0159-y, 2009.
Stone, E. L., and Kalisz, P. J.: On the maximum extent of tree roots, Forest Ecology and Management, 46, 59-102, https://doi.org/10.1016/0378-1127(91)90245-Q, 1991.
Terwilliger, V. J., and Waldron, L. J.: Effects of root reinforcement on soil-slip patterns in the Transverse Ranges of southern California, GSA Bulletin, 103, 775-785, https://doi.org/10.1130/0016-7606(1991)103<0775:Eorros>2.3.Co;2, 1991.
Thiebes, B., Bell, R., Glade, T., Jäger, S., Mayer, J., Anderson, M., and Holcombe, L.: Integration of a limit-equilibrium model into a landslide early warning system, Landslides, 11, 859-875, https://doi.org/10.1007/s10346-013-0416-2, 2014.
Uhlemann, S., Chambers, J., Wilkinson, P., Maurer, H., Merritt, A., Meldrum, P., Kuras, O., Gunn, D., Smith, A., and Dijkstra, T.: Four-dimensional imaging of moisture dynamics during landslide reactivation, Journal of Geophysical Research: Earth Surface, 122, 398-418, https://doi.org/10.1002/2016JF003983, 2017.
van Beek, R., Cammeraat, E., Andreu, V., Mickovski, S. B., and Dorren, L.: Hillslope Processes: Mass Wasting, Slope Stability and Erosion, in: Slope Stability and Erosion Control: Ecotechnological Solutions, edited by: Norris, J. E., Stokes, A., Mickovski, S. B., Cammeraat, E., van Beek, R., Nicoll, B. C., and Achim, A., Springer Netherlands, Dordrecht, 17-64, https://doi.org/10.1007/978-1-4020-6676-4_3, 2008.
Van Den Eeckhaut, M., Verstraeten, G., and Poesen, J.: Morphology and internal structure of a dormant landslide in a hilly area: The Collinabos landslide (Belgium), Geomorphology, 89, 258-273, https://doi.org/10.1016/j.geomorph.2006.12.005, 2007.
Van Den Eeckhaut, M., Muys, B., Van Loy, K., Poesen, J., and Beeckman, H.: Evidence for repeated re-activation of old landslides under forest, Earth Surface Processes and Landforms, 34, 352-365, https://doi.org/10.1002/esp.1727, 2009.

Vergani, C., Chiaradia, E. A., Bassanelli, C., and Bischetti, G. B.: Root strength and density decay after felling in a Silver Fir-Norway Spruce stand in the Italian Alps, Plant Soil, 377, 63-81, https://doi.org/10.1007/s11104-013-1860-4, 2014.

Vergani, C., and Graf, F.: Soil permeability, aggregate stability and root growth: a pot experiment from a soil bioengineering perspective, Ecohydrology, 9, 830-842, https://doi.org/10.1002/eco.1686, 2016.

Vergani, C., Schwarz, M., Soldati, M., Corda, A., Giadrossich, F., Chiaradia, E. A., Morando, P., and Bassanelli, C.: Root reinforcement dynamics in subalpine spruce forests following timber harvest: a case study in Canton Schwyz, Switzerland, Catena, 143, 275-288, https://doi.org/10.1016/j.catena.2016.03.038, 2016.

Vergani, C., Giadrossich, F., Buckley, P., Conedera, M., Pividori, M., Salbitano, F., Rauch, H. S., Lovreglio, R., and Schwarz, M.: Root reinforcement dynamics of European coppice woodlands and their effect on shallow landslides: A review, Earth-Sci. Rev., 167, 88-102, https://doi.org/10.1016/j.earscirev.2017.02.002, 2017.

Waldron, L. J.: The Shear Resistance of Root-Permeated Homogeneous and Stratified Soil, Soil Science Society of America Journal, 41, 843-849, https://doi.org/10.2136/sssaj1977.03615995004100050005x, 1977.

Wilfing, L., Meier, C., Boley, C., and Pfeifer, T.: Monitoring and analysis of a large mass movement area in clay endangering a motorway in Bavaria, Germany, ISRM European Rock Mechanics Symposium-EUROCK 2018, 2018.

Wu, T. H., McKinnell Iii, W. P., and Swanston, D. N.: Strength of tree roots and landslides on Prince of Wales Island, Alaska, Canadian Geotechnical Journal, 16, 19-33, https://doi.org/10.1139/t79-003, 1979.

Wu, T. H.: Effect of vegetation on slope stability, Transportation Research Record, 965, 37-46, 1984.

Young, R., xa, W, Wray, R., xa, A, xa, and L: Contribution to the Theory of Scarpland Development from Observations in Central Queensland, Australia, The Journal of Geology, 108, 705-719, https://doi.org/10.1086/317949, 2000.

Young, R. W.: Blockgliding in sandstones of the southern Sydney Basin, in: Aspects of Australian sandstone landscapes. Australian and New Zealand Geomorphology Group Special Publication 1, edited by: Young, R. W., and Nanson, G. C., 31-38, 1983.

Zhu, J., Wang, Y., Wang, Y., Mao, Z., and Langendoen, E. J.: How does root biodegradation after plant felling change root reinforcement to soil?, Plant Soil, 446, 211-227, https://doi.org/10.1007/s11104-019-04345-x, 2020.

Ziemer, R. R.: The role of vegetation in the stability of forested slopes, Proceedings of the International Union of Forestry Research Organizations, XVII World Congress, 6-17 September 1981, Kyoto, Japan. vol. I: 297-308, 1981.